Journal of the Korean Nuclear Society
Volume 35, Number 1, pp.14~24, February, 2003

Sintering Behavior of Cr_2O_3-doped UO_2 Pellets

Keon Sik Kim*†, Kun Woo Song*, Jae Ho Yang*, Ki Won Kang*, and Youn Ho Jung*
Korea Atomic Energy Research Institute
150 Dukjin-dong, Yuseung-gu, Daejeon 305-353, Korea

Gil Moo Kim†
Department of Materials Engineering, Chungnam National University
220 Gung-dong, Yuseong gu, Daejon 305-764, Korea

(Received June 26, 2002)

Abstract

This work investigates the effects of Cr_2O_3 and oxygen potential on grain growth and densification of UO_2 pellets. Powder mixtures of UO_2 and 0.03-0.4wt% Cr_2O_3 were pressed and sintered in 3 different gas atmospheres: the H_2O-to-H_2 ratios were 5×10^{-4}, 1×10^{-2} and 3×10^{-2}. In the first gas atmosphere the Cr_2O_3 contents below 0.2 wt% have an insignificant effect on grain size, but the Cr_2O_3 contents more than 0.3 wt% promote grain growth in the inner zone of a pellet but not in the outer zone. In both the second and third atmospheres, the grain size increases with the Cr_2O_3 content. With the same level of Cr_2O_3 content the grain size is larger in the second atmosphere than in the third. Sintering behavior and developed microstructure are discussed in terms of the reduction of Cr_2O_3 to Cr, the dissolution of Cr_2O_3 in UO_2, and liquid phase sintering.

Key Words : UO_2 fuel, sintering, Cr_2O_3, oxygen potential, duplex grain

1. Introduction

Uranium dioxide fuel with large grains can reduce the amount of fission gas released during irradiation [1], so it has been considered as desirable at high burnup. Various methods to make large-grained pellets are available: additives, higher sintering temperature, longer sintering time, and oxidizing atmosphere. Of the above methods the usage of additives has been widely studied, and thus the additives such as Nb_2O_5 [2,3,4], TiO_2 [2,5], MgO [6] and Cr_2O_3 [6] have been known to promote grain growth in sintering UO_2 pellets. Sintering behavior of additive-doped UO_2 is generally well known, but that of Cr_2O_3-doped UO_2 is fairly rarely studied. Kileen [7] prepared 0.5wt% Cr_2O_3-doped UO_2 pellets with a grain size of 50-55 μm and performed irradiation tests. Recently, Dehaudt et al. [8] reported briefly that adding a very small amount of about 0.06 wt% Cr_2O_3 to UO_2 is enough to produce a grain size of 50 μm. Up to now a mechanism for the

grain growth in Cr_2O_3-doped UO_2 has been little known.

Previous work on sintering behavior of additive-doped UO_2 [3,6] has reported that the oxygen potential of sintering gas has a crucial effect on whether additives are dissolved in UO_2 or not. For example, it has been known [3] that the added Nb_2O_5 can reduce to NbO in dry hydrogen and then hardly dissolves in UO_2, giving rise to a negligible effect on grain growth. But in wet hydrogen Nb_2O_5 or NbO_2 can be easily dissolved and promotes grain growth. MgO dissolves in UO_2 and produces larger grains, only when the oxygen potential of sintering gas is high [6],

This work is undertaken to investigate a role of the oxygen potential in connection with Cr_2O_3 content in sintering UO_2 pellets. This paper describes the effects of oxygen potential and Cr_2O_3 content on the sintering behavior of Cr_2O_3-doped UO_2 fuel pellets. Mechanisms related to the grain growth in Cr_2O_3-doped UO_2 are discussed in terms of liquid phase sintering or defects formed by the dissolved Cr_2O_3.

2. Experimental

The UO_2 powder used in this work was produced through the AUC (Ammonium Uranyl Carbonate) process [9]. The UO_2 powder has an O/U ratio of 2.1 and a BET surface area of 5 m^2/g. The average particle size was 17 μm. Cr_2O_3 powder was added to UO_2 powder, and two powders were then mixed for 20 min in a tumbling mixer. This powder mixture was further mixed using a sieve-mixing technique, which involved passing the powder mixture three times through a 140 mesh-sieve. The Cr_2O_3 contents of the powder mixtures were 0.03, 0.05, 0.1, 0.2 and 0.4 % by weight.

The powder mixture was pressed into green pellets of a density of about 5.7 g/cm^3. Green pellets were heated at a rate of 300℃/h and then held at 1700℃ for 4 h before furnace cooling. Three kinds of mixed gases consisting of hydrogen (H_2) and water vapor (H_2O) were used as sintering gases. Hydrogen gas has a dew point of -30℃, and thus has inherently a H_2O-to-H_2 ratio of 5.0×10^{-4}. Hydrogen gas passed a water bath set to a ceratin temperature, so it was saturated with water vapor before entering the sintering furnace. The H_2O-to-H_2 ratios in sintering gases were controlled to be 5×10^{-4}, 1×10^{-2} and 3×10^{-2}: these sintering gases will be termed "A-type", "B-type" and "C-type atmosphere", respectively, in the next part of this paper.

The gas mixture of hydrogen and water vapor reacts in thermodynamic equilibrium at elevated temperatures as follows :

$$2H_2O \rightarrow 2H_2 + O_2$$

The resultant composition of a gas mixture is determined by the equilibrium constant, which is a function of the temperature of gases. The SOLGASMIX program [10], which can calculate the Gibbs free energy and equilibrium constant of a reaction, was used to calculate the oxygen partial pressures of the sintering atmospheres under a total gas pressure of 1 bar.

The sintered density was determined by the water immersion method, and the theoretical density of Cr_2O_3-doped UO_2 was assumed to be 10.96 g/cm^3 like that of pure UO_2. Sintered pellets were sectioned longitudinally and polished. In order to observe grain boundaries thermal etching was carried out at 1250℃ for 1 h in carbon dioxide gas, and then grain size was determined by the linear intercept method.

In order to study the dependence of densification on temperature, the shrinkage of green pellets was measured in an axial direction with a linear variable differential transformer (LVDT) transducer

in a push-rod type dilatometer. UO_2 green pellets containing 0.2 wt% Cr_2O_3 were heated to 1650℃ at a rate of 5℃/min and then held 4 h. This shrinkage experiment used the same gas atmospheres as the sintering experiment.

3. Results

Fig. 1 shows the relations between the density of UO_2 pellets and Cr_2O_3 content for different H_2O-to-H_2 ratios in sintering atmospheres. In the A-type atmosphere ($H_2O/H_2=5\times10^{-4}$), the sintered density is nearly independent of Cr_2O_3 content. In B-type or C-type atmosphere ($H_2O/H_2=1\times10^{-2}$ or 3×10^{-2}), the density of UO_2 pellets substantially increases with the Cr_2O_3 content in the range of 0.2 wt% Cr_2O_3, and thereafter it decreases or levels off with further Cr_2O_3 contents. It is found that the magnitude of density increase is largest in the B-type atmosphere.

Figs. 2(a) and 2(b) show the microstructures of outer and inner zones of the 0.2wt% Cr_2O_3-doped pellet sintered in A-type atmosphere. Flake-like pores are commonly observed which are peculiar to the UO_2 pellet sintered using the UO_2 powder

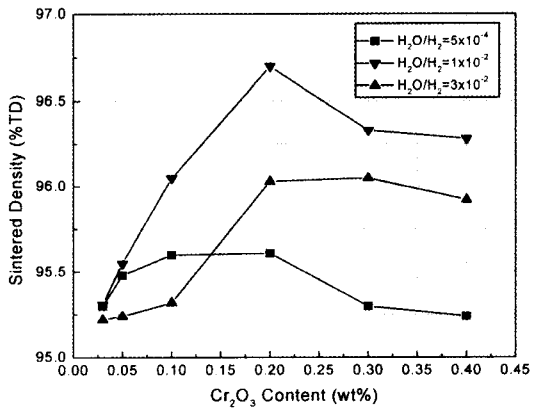

Fig. 1. Relations Between Sintered Density and Cr_2O_3 Content for Different H_2O-to-H_2 Ratios in Sintering Atmospheres

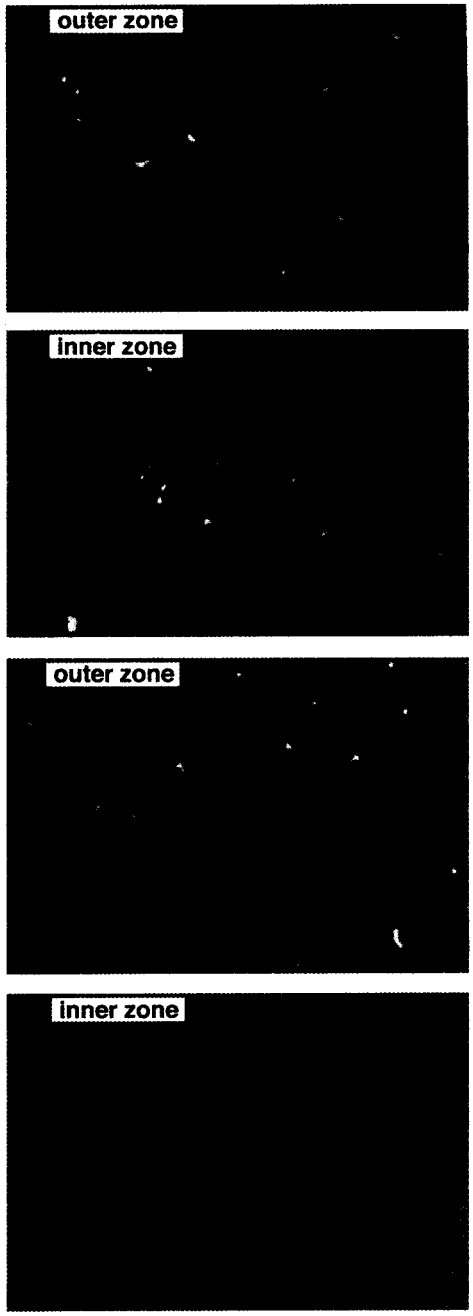

Fig. 2. Microstructures of Cr_2O_3-doped UO_2 Pellets Sintered in A-type Atmosphere which has a H_2O-to-H_2 Ratio of 5×10^{-4}:
(a) 0.2 wt% Cr_2O_3 and outer zone;
(b) 0.2 wt% Cr_2O_3 and inner zone;
(c) 0.3 wt% Cr_2O_3 and outer zone;
(d) 0.3 wt% Cr_2O_3 and inner zone

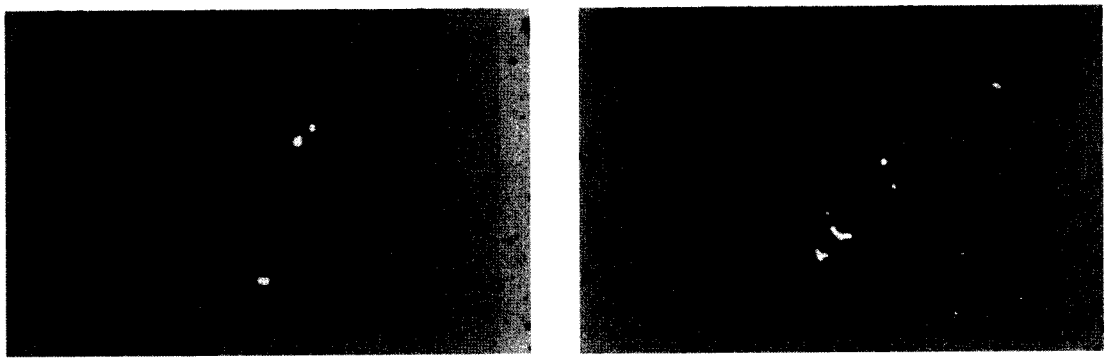

Fig. 3. Microstructures of Cr_2O_3-doped UO_2 Pellets Sintered in B-type Atmosphere which has a H_2O-to-H_2 Ratio of $1x10^{-2}$:
(a) 0.2 wt% Cr_2O_3; (b) 0.3 wt% Cr_2O_3

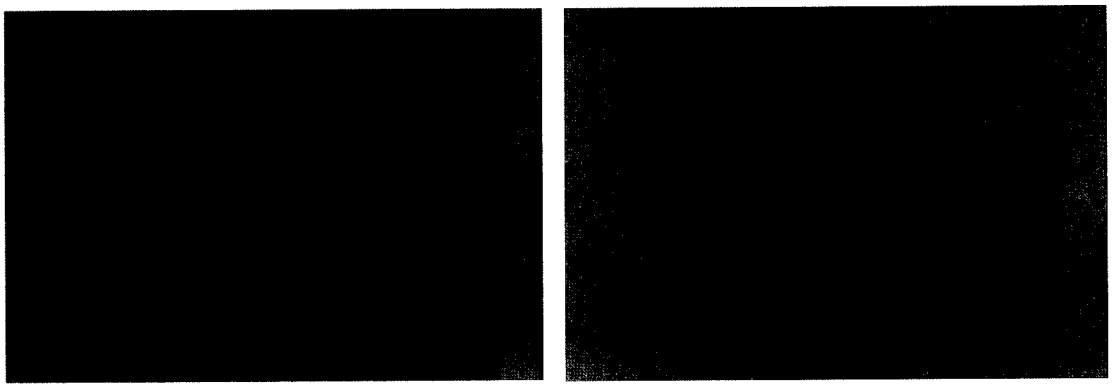

Fig. 4. Microstructures of Cr_2O_3-doped UO_2 Pellets Sintered in C-type Atmosphere which has a H_2O-to-H_2 ratio of 3×10^{-2}:
(a) 0.2 wt% Cr_2O_3; (b) 0.3 wt% Cr_2O_3

ex-AUC [11]. Metallic Cr precipitates (white particles) are found in both inner and outer zones, suggesting that Cr_2O_3 reduces to Cr over the whole pellet when the H_2O-to-H_2 ratio equals to 5×10^{-4}. However, when the level of Cr_2O_3 content rises to 0.3 or 0.4 wt%, metallic Cr precipitates form only in the outer zone but not in the inner zone. As an example, the microstructures of the outer and inner zones of a 0.3 wt% Cr_2O_3-doped pellet are shown in Figs. 2(c) and 2(d), respectively.

Figs. 3(a) and 3(b) show the microstructures of 0.2 and 0.3 wt% Cr_2O_3-doped pellets sintered in the B-type atmosphere ($H_2O/H_2=1 \times 10^{-2}$). These pellets are homogeneous in Cr precipitation over the whole pellet. A comparison between Fig. 3(a) and Fig. 2(a) indicates that even at the same Cr_2O_3 addition Cr precipitates form with much smaller amounts in the B-type atmosphere than in the A-type atmosphere. This indicates that the dissolution of Cr_2O_3 in UO_2 is quite dependent on the oxygen potential of sintering atmospheres.

Figs. 4(a) and 4(b) show the microstructures of 0.2 and 0.3 wt% Cr_2O_3-doped pellets, respectively, in C-type atmosphere ($H_2O/H_2=3 \times 10^{-2}$). Metallic Cr precipitates are not found in the microstructure while some chromic oxides remain

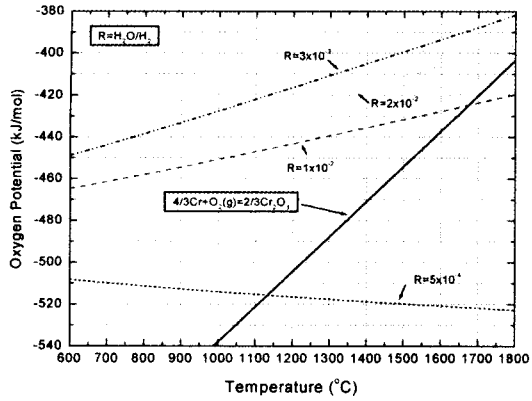

Fig. 5. Temperature Dependence of Oxygen Potentials of Sintering Atmospheres and Chromic Oxide

undissolved.

The microstructures in Figs. 2 to 4 suggest that the oxidation state of Cr varies sensitively with the slight changes in H_2O-to-H_2 ratio. Fig. 5 shows the oxygen potentials (RT ln $P(O_2)$) of sintering gases and chromic oxide as a function of temperature. The equilibrium line between Cr and Cr_2O_3 determines which of Cr_2O_3 or Cr is stable; Cr_2O_3 is stable in the left upper region of that line, but Cr is stable in the right lower region. During a temperature rise, Cr_2O_3 can begin to reduce to metallic Cr at about 1140℃ in the A-type atmosphere ($H_2O/H_2=5\times10^{-4}$) and at 1670℃ in B-type atmosphere ($H_2O/H_2=1\times10^{-2}$). Thus the Cr_2O_3 phase, which can be dissolved in UO_2, remains up to much higher temperatures in B-type than in A-type atmosphere; consequently, the added Cr_2O_3 dissolves in UO_2 more greatly in B-type atmosphere. This thermodynamic prediction is in good agreement with the experimental results that more Cr precipitates form in A-type atmosphere. In C-type atmosphere ($H_2O/H_2=3\times10^{-2}$), Cr_2O_3 is always stable compared to metallic Cr, so that the microstructure in Fig. 4 has no metallic Cr precipitates.

Fig. 6(a) shows the shrinkage (densification) of

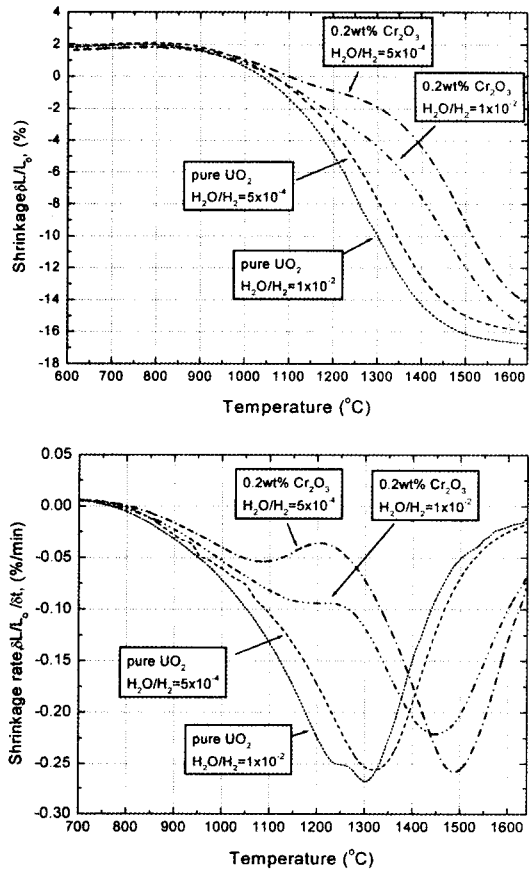

Fig. 6. Densification curves of UO_2 Green Pellets with and without 0.2 wt% Cr_2O_3 in A-type and B Type Atmospheres: (a) densification; (b) densification rate

0.2 wt% Cr_2O_3-doped UO_2 green pellets as a function of temperature in A-type and B-type atmospheres. Fig. 6(b) shows the shrinkage rates derived from the shrinkage in Fig. 6(a). For comparison the shrinkage of pure UO_2 green pellets is shown together. UO_2 green pellets with and without Cr_2O_3 start to densify at about 800℃. But Cr_2O_3-doped UO_2 green pellets densify less than pure UO_2 above 1000°... since Cr_2O_3 particles placed between UO_2 particles might, early in sintering, prohibit sintering between UO_2 and UO_2 particles. Over a temperature range

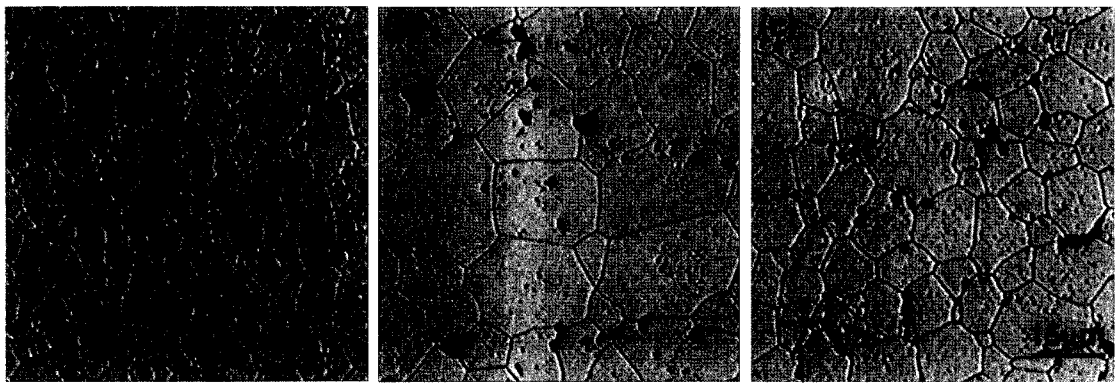

Fig. 7. Grain Structures of 0.2 wt% Cr_2O_3-doped UO_2 Pellets Sintered in Different Atmospheres: (a) A-type; (b) B-type; (c) C-type

between 1150 and 1300℃ the densification of a Cr_2O_3-doped UO_2 is strongly suppressed in A-type atmosphere, and a similar suppression also occurs with a lesser extent in B-type atmosphere.

Such suppression in densification might be related with two factors: the reduction of Cr_2O_3 to Cr and the dissolution of Cr_2O_3 in UO_2. As shown in Fig. 2(a), Cr_2O_3 reduces to Cr in A-type atmosphere. The density of Cr_2O_3 (5.22 g/cm^3) is much smaller than that of Cr (7.19 g/cm^3). Thus the reduction might cause volume contraction, with new pores forming just near Cr precipitates. These new pores can lead to suppression in densification. On the other hand, the dissolution of Cr_2O_3 in UO_2 needs both Cr ion diffusion from Cr_2O_3 particles to the surrounding UO_2 and U ion diffusion with the reverse direction. The amount of Cr ion which diffuses out to the surrounding UO_2 should be much larger than that of U ion which diffuses into the Cr_2O_3 particle, because the Cr ion concentration should be uniform over the whole UO_2 pellet. Accordingly, Cr ion might diffuse directionally to the surrounding UO_2, with new pores forming at the original places of Cr_2O_3 particles by the Kirkendall effect. Recently, Song et al. [12] have found that new pores form as a result of the dissolution of Gd_2O_3 in UO_2. The pore formation due to the reduction of Cr_2O_3 to Cr might mainly act in suppressing densification in A-type atmosphere, but the pore formation due to the dissolution of Cr_2O_3 in UO_2 might mainly act in the B-type atmosphere.

Fig. 6(b) shows that the relation between densification rate and temperature is affected by the Cr_2O_3 addition. The densification rate of UO_2 pellets increases with temperature up to about 1300℃ and then decreases; consequently, it has a peak value near 1300℃. The densification rate of Cr_2O_3-doped UO_2 pellets undergoes a decrease or a suspension over a temperature range between 1100 and 1250℃ and has a peak value near 1450℃. Thus Cr_2O_3 addition makes densification rate decline at low temperatures but rise at high temperatures.

Figs. 7(a), 7(b) and 7(c) show the microstructures of 0.2wt% Cr_2O_3-doped UO_2 pellets sintered in A-type, B-type and C-type atmospheres, respectively. The grain size is largest in B-type atmosphere ($H_2O/H_2=1\times10^{-2}$). The grain structures of 0.2wt% Cr_2O_3-doped UO_2 pellets are uniform in all the atmospheres; however, nonuniform grain structure develops in 0.3wt% or 0.4wt% Cr_2O_3-doped pellets sintered in A-type atmosphere. It is found that the grain size is about

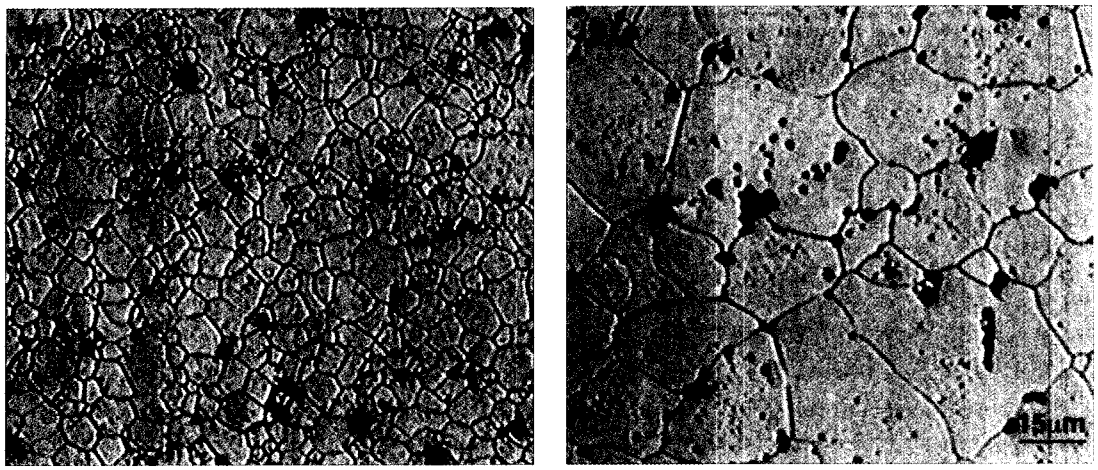

Fig. 8. Inhomogeneous Grain Structures Formed by Sintering a 0.4wt% Cr_2O_3-doped UO_2 Pellet in A-type Atmosphere:
(a) outer zone; (b) inner zone

3-4 times larger in the inner zone of a pellet than in the outer zone. This duplex grain structure of the 0.4wt% Cr_2O_3-doped pellet is shown in Figs. 8(a) and 8(b), which represent outer and inner zones of a pellet, respectively. The outer zone is very similar in size to the outer zone where metallic Cr precipitates are formed (see Fig. 2(c)). So inhomogeneity in the grain structure might be associated with inhomogeneity in metallic Cr precipitation.

The relations between grain size and Cr_2O_3 content for various sintering atmospheres are given in Fig. 9. In A-type atmosphere ($H_2O/H_2=5\times10^{-4}$), the grain size remains almost constant as far as the Cr_2O_3 content is lower than 0.2wt%, and thereafter the grain size in the inner zone increases with the Cr_2O_3 content while the grain size in the outer zone still remains constant. In C-type atmosphere ($H_2O/H_2=3\times10^{-2}$), the grain size increases with the Cr_2O_3 content and then levels off with Cr_2O_3 contents higher than 0.2 wt%. In B-type atmosphere ($H_2O/H_2=1\times10^{-2}$), the grain size increases progressively with the Cr_2O_3 content and thus reaches about 27 μm at 0.4 wt% Cr_2O_3.

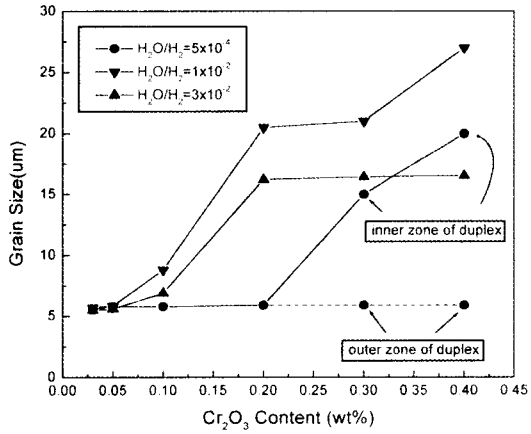

Fig. 9. Relations Between Grain Size and Cr_2O_3 Content for Different H_2O-to-H_2 Ratios in Sintering Atmospheres

The grain size is largest in B-type atmosphere as the sintered density is.

Fig. 10 shows the dependence of lattice parameter on Cr_2O_3 content for UO_2 pellets sintered in different atmospheres. The atmosphere which has a H_2O-to-H_2 ratio of 1.5×10^{-2} has been chosen due to its sufficient oxygen potential for the inhibition of the reduction of Cr_2O_3 to Cr

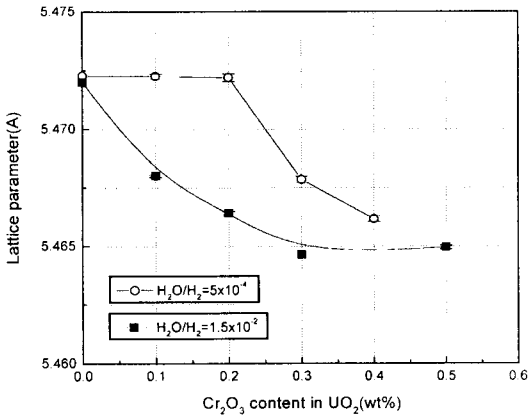

Fig. 10. Variations in Lattice Parameter of Cr_2O_3-doped UO_2 with Cr_2O_3 Content for Different Atmospheres

during sintering. In this atmosphere the lattice parameter declines with the Cr_2O_3 content and then remains almost constant with Cr_2O_3 contents higher than 0.3 wt%. The dissolution of Cr_2O_3 in UO_2 leads a decreases in the lattice parameter of UO_2, and the amount of this decrease is proportional to the Cr_2O_3 content dissolved. The solubility limit of Cr_2O_3 in UO_2 might be around 0.3 wt% Cr_2O_3 in this atmosphere.

In the A-type atmosphere the lattice parameter remains constant with the Cr_2O_3 content in the range of 0.2 wt%, but it declines with larger Cr_2O_3 contents. The declining rate of lattice parameter is similar in both atmospheres. It is supposed that large amounts of Cr_2O_3 addition -0.3 and 0.4 wt%- can produce some dissolution of the added Cr_2O_3 while small amounts of Cr_2O_3 addition fail to dissolve in UO_2. This dissolution behavior of Cr_2O_3 in A-type atmosphere is in good agreement with the findings in microstructure; metallic Cr precipitates form over the whole pellet with the Cr_2O_3 contents smaller than 0.2 wt%, but metallic Cr precipitates form only in the outer zone of pellets containing Cr_2O_3 contents larger than 0.3 wt%.

4. Discussions

4.1. Formation of Duplex Grain Structure

In the A-type atmosphere grain growth in UO_2 is insignificantly affected by the Cr_2O_3 addition level lower than 0.2 wt% because Cr_2O_3 reduces to Cr before dissolving in UO_2. However, grain growth is enhanced locally by the addition of 0.3 wt% or 0.4 wt% Cr_2O_3 and thus leads to the formation of a duplex grain structure - large grains in the inner zone of a pellet and small grains in the outer zone. It was also found that metallic Cr precipitates form in the outer zone but not in the inner zone.

According to the thermodynamic calculation (see Fig. 5), Cr_2O_3 begins to reduce to Cr at about 1140℃ in the A-type atmosphere. This reduction theoretically occurs simultaneously over the whole pellet. In reality, however, the reduction might occur earlier or faster in the outer zone than in the inner zone, probably because of differences in temperature and oxygen potential between the two zones during heating.

Since heat provided flows from the outer zone to the inner zone, the temperature is always lower in the inner zone than in the outer zone during heating. Thus it is reasonable to expect that the Cr_2O_3 in the outer zone reduces to Cr earlier than the Cr_2O_3 in the inner zone during temperature rise. On the other hand, the reduction of Cr_2O_3 might be also affected by changes in the oxygen potential of sintering gas. During temperature rise the O/U ratio of a green pellet should decrease from 2.10 to 2.0. This decrease in the O/U ratio generates oxygen, which combines with hydrogen to produce steam (water vapor). The steam produced in the outer zone escapes from a pellet with ease due to the fact that the outer zone is exposed to the pellet surface. But the steam in the

inner zone might escape with more difficulty because of limited flow channels. Therefore, it is possible that the oxygen potential is temporarily higher in the inner zone during temperature rise, and this increase in oxygen potential might also delay the reduction of Cr_2O_3 in the inner zone.

Once the reduction of Cr_2O_3 occurs preferentially in the outer zone, the oxygen derived from Cr_2O_3 might combine with hydrogen to produce steam. Part of the generated steam escapes from the pellet, and much of the rest might flow into the inner zone. Thus a gas atmosphere in the inner zone may get extra H_2O content, and a rise in the H_2O-to-H_2 ratio keeps Cr_2O_3 stable up to higher temperatures (see Fig. 5). The Cr_2O_3 phase can be dissolved in UO_2, but metallic Cr might not. When Cr_2O_3 addition is smaller than 0.2 wt%, the amount of H_2O gas that has flown into the inner zone may be too small to raise the H_2O-to-H_2 ratio to such an extent that the reduction in the inner zone is inhibited. However, when Cr_2O_3 addition is greater than 0.3wt%, the amount of H_2O gas that has flown into the inner zone might be enough to provide a higher H_2O-to-H_2 ratio for the inhibition of the reduction of Cr_2O_3. Thus Cr_2O_3 can be dissolved only in the inner zone, with metallic Cr precipitates forming in the outer zone. This inhomogeneous dissolution of Cr_2O_3 may cause a duplex grain structure to form.

4.2. Mechanisms for the Grain Growth

The addition of Cr_2O_3 to UO_2 enhances grain growth in B-type and C-type atmospheres, with the magnitude of this enhancement increasing with the Cr_2O_3 content. The dissolved Cr_2O_3 might increase uranium diffusion which is a controlling step in sintering UO_2.

The dissolved Cr ions in UO_2 structure will generate new defects such as oxygen vacancy or oxygen interstitial since a dominant defect is anion-Frenkel defect in UO_2. If the entrance of Cr ions generates oxygen vacancies to maintain electrical neutrality, this increase in oxygen vacancy concentration will lead to a decrease in uranium vacancy concentration through Schottky equilibrium. Eventually, the dissolved Cr ion results in a decrease in uranium diffusion. This explanation is inconsistent with the results that the dissolved Cr_2O_3 enhances grain growth during sintering.

Alternatively, if oxygen interstitials are generated by the entrance of Cr ions, an increase in oxygen interstitial concentration will result in a decrease in oxygen vacancy concentration through Frenkel equilibrium. And, in turn, uranium vacancy concentration comes to increase through Schottky equilibrium; consequently, uranium diffusion is accelerated by an increase in uranium vacancy concentration. This increase in uranium diffusion is in good agreement with the rise in grain size (see Fig. 9). Therefore, it can be inferred that the dissolution of Cr_2O_3 in UO_2 generates oxygen interstitials.

The influence of Cr_2O_3 addition on grain growth is proven to be dependent on the oxygen potential of sintering gases. At the same level of Cr_2O_3 addition, grain growth is more greatly enhanced in the B-type atmosphere ($H_2O/H_2 = 1\times10^{-2}$) than in C-type atmosphere ($H_2O/H_2 = 3\times10^{-2}$). Since Cr_2O_3 can dissolve in UO_2 in both atmospheres, this difference in sintering behavior suggests that not only the dissolved Cr_2O_3 but also other factors operate in sintering Cr_2O_3-doped UO_2.

Fig. 5 indicates that Cr_2O_3 begins to reduce to Cr at about 1670℃ in the B-type atmosphere. The remaining Cr_2O_3 that have not been dissolved during the temperature rise of up to 1670℃ reduces to Cr in B-type atmosphere, so that both Cr_2O_3 and Cr can exist together above this temperature. According to the phase diagram for Cr-Cr_2O_3 system [13], Cr and Cr_2O_3 make an

Fig. 11. Microstructure of a 1 wt% Cr_2O_3-doped UO_2 Pellet Sintered in B-type Atmosphere

eutectic reaction to form a liquid at 1645℃, and thus (liquid), (Cr_2O_3 + liquid) and (Cr + liquid) phases are present above 1645℃ over the whole composition range. It is difficult to observe a trace of liquid phase in the 0.4 wt% Cr_2O_3-doped UO_2 pellet. But traces of liquid phase can be easily identified in pellets containing more Cr_2O_3 content. Fig. 11 illustrates a second phase which forms at the grain corners or on the grain boundaries in the 1 wt% Cr_2O_3-doped UO_2 pellet sintered in B-type atmosphere. The second phase is indicated by the arrows in Fig. 11. The microstructure is characterized by round grains of UO_2 and small dihedral angles of the second phase, suggesting that the second phase was once a liquid phase during sintering. Wavelength dispersive X-ray analysis of the second phase reveals that it consists of Cr_2O_3 and 2.4 atomic % UO_2, suggesting that UO_2 was soluble in a liquid phase during sintering. If liquid phase sintering occurs in B-type atmosphere, material transport needed in sintering UO_2 can be accelerated through the liquid phase. It is well known that liquid phase sintering enhances greatly grain growth in sintering TiO_2-doped UO_2 [5]. Therefore, not only the dissolved Cr_2O_3 but also liquid phase sintering enhances grain growth in B-type atmosphere. In C-type atmosphere, however, the dissolved Cr_2O_3 solely enhances grain growth.

4. Conclusions

Grain growth in Cr_2O_3-doped UO_2 is essentially dependent on the oxygen potential of sintering atmospheres. In A-type atmosphere which has a H_2O-to-H_2 ratio of 5×10^{-4}, the Cr_2O_3 addition smaller than 0.2 wt% has a negligible effect on grain growth because Cr_2O_3 reduces to Cr above about 1100℃ before dissolving. However, the Cr_2O_3 addition larger than 0.3 wt% leads to the formation of a duplex grain structure - small grains in the outer zone of a pellet and large grains in the inner zone. This inhomogeneity in grain size can be attributed to the fact that Cr_2O_3 reduces to Cr before dissolving in the outer zone but dissolves in UO_2 in the inner zone. In a heating stage during sintering, the reduction of Cr_2O_3 to Cr might occur earlier in the outer zone, and part of the reduction product that is mainly steam may flow into the inner zone. The oxygen potential of sintering gas can rise locally in the inner zone; consequently, the Cr_2O_3 phase which is favourable for dissolving in UO_2 remains in the inner zone as a result of the reduction of Cr_2O_3 to Cr in the outer zone. Eventually, the dissolution of Cr_2O_3 occurs preferentially in the inner zone during sintering.

In B-type and C-type atmosphere which have H_2O-to-H_2 ratios of 1×10^{-2} and 3×10^{-2}, respectively, the grain size and sintered density increases with the dissolved Cr_2O_3 content. The magnitude of the increase in grain size is larger in B-type atmosphere than in C-type atmosphere. Cr_2O_3 begins to reduce to Cr at about 1670℃ in a heating stage in B-type atmosphere, and then a liquid phase forms through an eutectic reaction between Cr_2O_3 and Cr. Material transport for

grain growth can be accelerated through this liquid phase. Both the dissolved Cr_2O_3 and liquid phase sintering act in B-type atmosphere, but only the dissolved Cr_2O_3 does in C-type atmosphere.

Acknowledgements

This work has been carried out under the Nuclear R & D Program supported by the Ministry of Science and Technology, Korea.

References

1. J.A. Turnbull, J. Nucl. Mater. 50 (1974) 62.
2. K.C. Radford and J.M. Pope, J. Nucl. Mater. 116, 305 (1983).
3. K.W. Song, K.S. Kim, K.W. Kang and Y.H. Jung, J. Korean Nucl. Soc. 31, 335 (1999).
4. Y. Harada, J. Nucl. Mater. 238, 237 (1997).
5. J.B. Ainscough, F. Rigby and S.C. Osborn, J. Nucl. Mater. 52, 191 (1974).
6. B.E. Ingleby and K. Hand, in: Fission- Product Behavior in Ceramic Oxide Fuel, ed. I.J. Hastings, (Am. Ceramic Soc., 1986), Advances in Ceramics, vol. 17, p. 57.
7. J.C. Kileen, J. Nucl. Mater. 88, 177 (1980).
8. P. Dehaudt, C. Lemaignan, L. Caillot, A. Mocellin and G. Eminet, in: Advances in Pellet Technology for Improved Performance at High Burnup (IAEA, Vienna, 1998), IAEA-TECDOC-1036, p. 27.
9. C.S. Choi, J.H. Park, E.H. Kim, H.S. Shin and I.S. Chang, J. Nucl. Mater. 153, 148 (1991).
10. HSC Chemistry for Windows 1994, Outokump research.
11. K.W. Song, K.S. Kim, Y.M. Kim, K.W. Kang and Y.H. Jung, J. Nucl. Mater. 279, 253 (2000).
12. K.W. Song, K.S. Kim, J.H. Yang, K.W. Kang and Y.H. Jung, J. Nucl. Mater. 288, 92(2001) .
13. R.E. Johnson and A. Muan, J. Amer. Ceram. Soc. 51, 430 (1968).